Astrophysical Masers:
Unlocking the Mysteries of the Universe
Proceedings IAU Symposium No. 336, 2017
A. Tarchi, M.J. Reid & P. Castangia, eds.

doi:10.1017/S1743921317010699

Sub-mm observations of periodic methanol masers

D. J. van der Walt[1], J.-M. Morgan[1], J. O. Chibueze[2,1,3] and Q. Zhang[4]

[1]Centre for Space Research, NWU, Potchefstroom, South Africa
email: johan.vanderwalt@nwu.ac.za, jeanmariemorgan0@gmail.com, jchibueze@ska.ac.za, qzhang@cfa.harvard.edu

[2]SKA-SA, Pinelands, South Africa;
[3]Dept. Physics & Astronomy, University of Nigeria, Nsukka, Nigeria; [4]Harvard-Smithsonian CfA, USA

Abstract. We present the results of sub-millimetre observations on three periodic methanol maser sources. Our results indicate that there are geometric differences between some periodic methanol masers which have different variability profiles.

Keywords. Stars:formation, ISM:molecules, submillimetre

1. Introduction

One of the fundamental questions about the periodic methanol masers concerns the driving mechanism underlying the periodic behaviour. The light curves of the periodic masers must in some way reflect the origin of the underlying physical mechanism (see eg. van der Walt *et al.* 2016). We observed G22.357+0.066 with a maser light curve similar to that of G9.62+0.20E, and G25.411+0.105 which has a maser light curve resembling a $|\sin(x)|$ curve to investigate whether there are obvious differences between these sources.

2. SMA observations and ALMA archival data

The target sources G22.357+0.066 and G25.411+00.105 were observed on June 27, 2016, during a 5-hour track with the Submillimeter Array (SMA) in a compact array configuration. The SMA $\sim$ 230 GHz broad band covered the dust continuum and the J = 2-1 spectral lines of ^{12}CO, ^{13}CO, C^{18}O, using 7 of the 8 antennas. The data calibration and imaging were done in CASA. We also obtained ALMA band 6 archival data on G9.62+0.20E (Project ID: 2013.1.00957.S). More details of these observations can be found in Liu, *et al.* (2017). The respective maps are shown in Figs. 1 & 2.

3. Results and Discussion

G22.357+0.066 (Fig. 1a): Comparison of the ^{13}CO emission (black contours) and the dust continuum (white contours) very strongly suggests that the detected ^{13}CO emission is not associated with the dust continuum emission. The masers (filled circle) also seem to be associated with the dust continuum rather than with the CO emission. Separate NIR counterparts (black triangles) for the CO and dust emission could be found from UKIDSS. The absence of ^{12}CO and ^{13}CO emission with the dust continuum is likely to be a density effect, suggesting that the masers are associated with a very young object.

G25.411+0.105 (Fig. 1b): The ^{13}CO line profile show strong blue- and redshifted wings, suggesting the presence of an outflow oriented in the direction of the line of

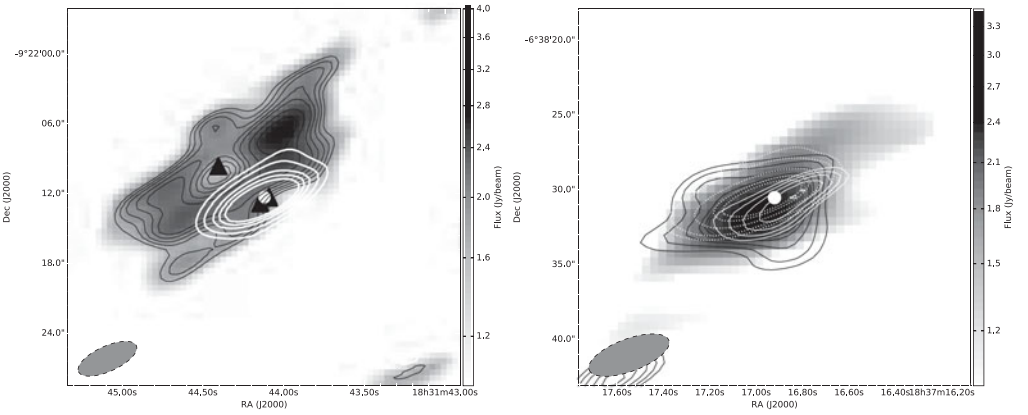

(a) G22.356+0.066 (b) G25.411+0.105

Figure 1. SMA maps of G22.357+0.066 and G25.411+0.105

sight. Strong ^{13}CO emission not associated with the outflow has also been detected (gray scale). The ^{13}CO emission indicates the presence of lower density gas which might suggest a somewhat later evolutionary phase than for G22.357+0.066. The masers are seen to be projected against the outflows. The maser spot distribution is elliptical and has been interpreted by Bartkiewicz *et al.* (2009) as being to due to a disk viewed almost face on. This is consistent with the direction of the outflows as shown in Fig. 1b.

G9.6+0.20E (Fig. 2): No clear ^{12}CO emission directly associated with the dust continuum (white contours) and with the 5_{-1}-4_{-2} E-CH_3OH (grayscale) emission, has been detected. A well defined bi-polar outflow has been detected in CO (black contours: red shifted, gray contours: blue shifted). The thermal E-CH_3OH emission is a high density tracer ($n_{cr} \sim 10^6$ cm^{-3}) and forms a thick structure with the dust continuum projected on the center of this structure. As in the case of G22.357+0.066, the absence of ^{12}CO emission might be a density effect.

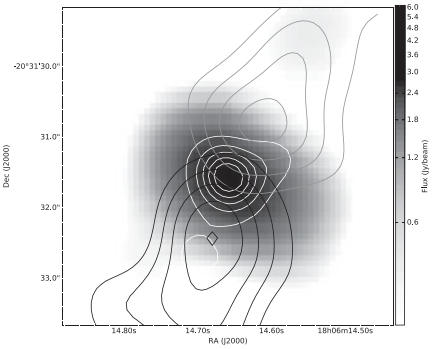

Figure 2. G9.62+0.20E

The first obvious difference between G9.62+0.20E and G25.411+0.105 (with maser light curves that are different) is clearly geometric, with G9.62+0.20E having outflows in the plane of the sky, while for G25.411+0.105 the line of sight is almost parallel to the outflow axis. In the case of G25.411+0.105 the periodic masers are projected onto the outflow; it is not clear whether it affects the maser light curve. For G22.357+0.066 and G9.62+0.20E the absence of ^{12}CO and ^{13}CO emission associated with the dust emission might indicate an earlier evolutionary phase than for G25.411+0.105.

References

Bartkiewicz, A., Szymczak, M., van Langevelde, H. J., *et al.* 2009, *A&A*, 502, 155
Liu, T., Lacy, J., Li, P. S., *et al.* 2017, *ApJ*, 849, 25
van der Walt, D. J., Maswanganye, J. P., Etoka, S. Goedhart, S., & van den Heever, S. P. 2016, *A&A*, 588, 47

https://doi.org/10.1017/S1743921317010699 Published online by Cambridge University Press